Analytical Model for Ion Acceleration by High-Intensity Laser Pulses

J. Schreiber,[1,2,*] F. Bell,[1] F. Grüner,[1] U. Schramm,[1] M. Geissler,[2] M. Schnürer,[3] S. Ter-Avetisyan,[3] B. M. Hegelich,[4] J. Cobble,[4] E. Brambrink,[5] J. Fuchs,[5] P. Audebert,[5] and D. Habs[1]

[1]*Department für Physik, Ludwig-Maximilians-Universität München, Garching, Germany*

[2]*Max-Planck-Institut für Quantenoptik, Garching, Germany*

[3]*Max-Born-Institut, Berlin, Germany*

[4]*Los Alamos National Laboratory, Los Alamos, New Mexico 87545, USA*

[5]*Laboratoire pour l'Utilisation des Lasers Intenses, UMR 7605, CNRS-CEA-École Polytechnique-Université Paris VI, Palaiseau, France*

(Received 2 May 2006; published 28 July 2006)

We present a general expression for the maximum ion energy observed in experiments with thin foils irradiated by high-intensity laser pulses. The analytical model is based on a radially confined surface charge set up by laser accelerated electrons on the target rear side. The only input parameters are the properties of the laser pulse and the target thickness. The predicted maximum ion energy and the optimal laser pulse duration are supported by dedicated experiments for a broad range of different ions.

DOI: 10.1103/PhysRevLett.97.045005 PACS numbers: 52.38.Kd, 41.75.Jv, 52.59.−f

Ion acceleration from high-intensity laser irradiated thin foils has attracted high attention during the past decade. The emitted ion and, in particular, proton pulses contain large particle numbers between 10^{10} and 10^{13} with energies in the MeV [1,2] and multi-MeV range [3–6] and are tightly confined in time (∼ps) and space (source radius a few μm). These outstanding characteristics triggered speculations about a wide range of applications in nuclear and medical physics.

The dependence of the ion spectra on the intensity [7,8] and target thickness was investigated experimentally [2,4,9]. Theoretical models are presently based on particle-in-cell simulations (PIC) [10,11] and plasma expansion models (PEM) [12,13], the physical picture of the process being the following. First, electrons are accelerated by the impinging relativistic laser pulse and penetrate the target driven by the Lorentz force. Leaving the target at the rear side, they set up a huge electric field which, in essence, is pointed normal to the target rear surface. Most electrons are forced to turn around and build up a quasistationary electron layer. By this field surface atoms are field ionized and accelerated. This process is called target normal sheath acceleration [10]. In most experiments, a thin layer (∼nm) of hydrocarbons, water, or oxides contaminates the target surfaces so that ions with the highest charge-to-mass ratio are accelerated predominantly.

In this work, we present a simple analytical model based solely on a radially confined surface charge set up by laser accelerated electrons on the target rear side. The model explains the maximum ion energies observed in a variety of existing experiments as well as in dedicated studies where either the laser pulse duration or the charge-to-mass ratio of the ions was varied.

We assume that N_e electrons are accelerated by the laser and confined in an electron bunch of length $L = c\tau_L$, where τ_L is the laser pulse duration. At the rear side of the foil, the electrons are transversely spread over a circular area with radius

$$B = r_L + d\tan\theta, \tag{1}$$

where r_L denotes the radius of the laser spot, d the thickness of the target, and θ the half-angle of the electrons traveling through the target. We further imply an exponential electron energy distribution

$$\frac{dN}{dE} = \frac{N_e}{k_B T_e}\exp\left[-\frac{E}{k_B T_e}\right]. \tag{2}$$

When electrons cross the solid-vacuum boundary, they induce a positive surface charge Qe on the conducting rear surface, leading to a surface charge density $Qe/(\pi B^2)$ located at $z = 0$, where z is the electron propagation axis. Solving the Poisson equation for such a charge density distribution, the potential on the z axis is given by

$$-e\Phi(\xi) = E_\infty s(\xi), \tag{3}$$

with $\xi = z/B$ and $s(\xi) = 1 + \xi - (1 + \xi^2)^{1/2}$. Only a few electrons with energies exceeding $E_\infty = Qe^2/(2\pi\epsilon_0 B)$ can escape the rear surface potential, whereas the low energetic electrons reenter the foil. The point $\hat{\xi} = \hat{z}/B$ where electrons with the mean energy $k_B T_e$ turn around is defined by $E_\infty s(\hat{\xi}) \approx E_\infty \hat{\xi} = k_B T_e$, for $\hat{\xi} \ll 1$. This approximation is valid for all experiments to be discussed. Using the definition for E_∞ and the electron density $n_{Q0} = Q/(\pi B^2 \hat{z})$ directly at the surface, one derives

$$\hat{z} = (2\epsilon_0 k_B T_e/n_{Q0}e^2)^{1/2} \equiv \lambda_D, \tag{4}$$

where λ_D is called the hot electron Debye length.

The electron density distribution which is in equilibrium with the surface charge potential Φ then reads

$$n_Q(\xi) = n_{Q0}\exp[-s(\xi)/\xi_D][1 - \xi/(1 + \xi^2)^{1/2}], \tag{5}$$

where $\xi_D = \lambda_D/B$. Electrons propagate over distance λ_D and back before they reenter the foil. This leads to an equilibrium situation where $Q = 2N_e\lambda_D/L$ electrons are permanently outside the foil, which, in turn, induce Q positive charges in order to maintain charge neutrality also on a scale of λ_D.

From Eq. (3) together with $F = -d\Phi/dz$, we obtain

$$F(\xi) = \frac{k_B T_e}{e\lambda_D}[1 - \xi/(1 + \xi^2)^{1/2}] \quad (6)$$

for the electric field F in the vacuum region outside the foil. Directly at the surface ($\xi = 0$), the electric field agrees with the well-known result $F_0 = k_B T_e/(e\lambda_D)$ from PEM [12,13]. Yet, in contrast to PEM, the potential [Eq. (3)] stays finite for $\xi \to \infty$ in our model.

In a second step, the potential equation (3) is used to calculate the energy $E_i(\xi)$ an ion with charge $q_i e$ gains between $\xi = 0$ and ξ

$$E_i(\xi) = -q_i e\Phi(\xi) = E_{i,\infty} s(\xi), \quad (7)$$

where $E_{i,\infty} = q_i k_B T_e B/\lambda_D$ defines the energy an ion with charge $q_i e$ could theoretically gain by completely running down the potential well. Here we describe only the most energetic ions which are emitted from the center of the emission zone where the field is highest. Ions starting from outer zones or from deeper surface layers ($z < 0$) will gain less energy and are not treated. The ion energy $E_i(\xi)$ of Eq. (7) results solely from the repulsion due to surface charges Qe; i.e., the influence of the hot electrons is neglected. This assumption is justified by the following simple picture based on the very different longitudinal spatial distributions of both charge contributions. The positive charge distribution (surface charges) is much more localized than the electron cloud n_Q above the rear surface. The electron center of charge is approximately at a distance λ_D above the surface, and its longitudinal width is of the same order. Thus, the forces of the electrons on an ion at some distance from the surface compensate each other to some degree.

Using the fact that the laser energy $E_L = P_L\tau_L$ is converted with an efficiency η into hot electron energy, i.e., $N_e k_B T_e = \eta E_L$, we derive

$$E_{i,\infty} = q_i 2mc^2(\eta P_L/P_R)^{1/2}, \quad (8)$$

where $P_R = mc^3/r_e = 8.71$ GW is the relativistic power unit (r_e is the classical electron radius). $E_{i,\infty}$ denotes the maximum possible energy an ion could gain for a certain laser power P_L providing an infinitely long acceleration. For radiation of the order of 1 μm wavelength, the efficiency can be approximated by $\eta = 1.2 \times 10^{-15} \cdot I_L^{3/4}$, with I_L in W/cm^2 [14,15] up to a maximum value of $\eta = 0.5$. This maximum conversion efficiency is reached for a laser intensity $I_L = P_L/(\pi r_L^2) = 3.1 \times 10^{19}$ W/cm^2, as indicated by Hatchett *et al.* [5] and successfully used by Fuchs *et al.* [16]. Note that the maximum possible ion energy depends on the square root of the absorbed laser pulse power only [17] and that Eq. (8) shows no explicit dependence on the hot electron temperature T_e.

For experimentally observable maximum ion energies E_m, we need to include the time dependence of the accelerating process, i.e., the stopping of the acceleration after the electron pulse has passed. This is expressed by integrating the equation of motion $d\xi/dt = v(\xi)/B$ with $v(\xi) = (2E_i(\xi)/m_i)^{1/2}$ [Eq. (7)] and m_i as the ion mass; one has

$$\frac{\tau_L}{\tau_0} = X\left(1 + \frac{1}{2}\frac{1}{1 - X^2}\right) + \frac{1}{4}\ln\frac{1 + X}{1 - X}, \quad (9)$$

where $\tau_0 = B/v(\infty)$ and $X = (E_m/E_{i,\infty})^{1/2}$. This Eq. (9) is the main result of our analysis and will be compared with experimental values. The data shown in Fig. 1 are divided into three groups with comparative laser pulse parameters in terms of energy and pulse duration. For the electron propagation angle θ [Eq. (1)], a value of 10° was estimated following Ref. [9] for the 1 J-laser group (ASTRA, ATLAS, MBI, LOA, JANUSP), of 25° as used in Ref. [16] and confirmed by source-size measurements [18] for the 10 J-laser group (GEKKO, LULI, TRIDENT), and of 45° for the 100 J-laser group (NOVAPW, RALVULCAN, RALPW) as indicated by angular resolved x-ray measurements [19]. A precise determination of the source size B seems to be difficult, and

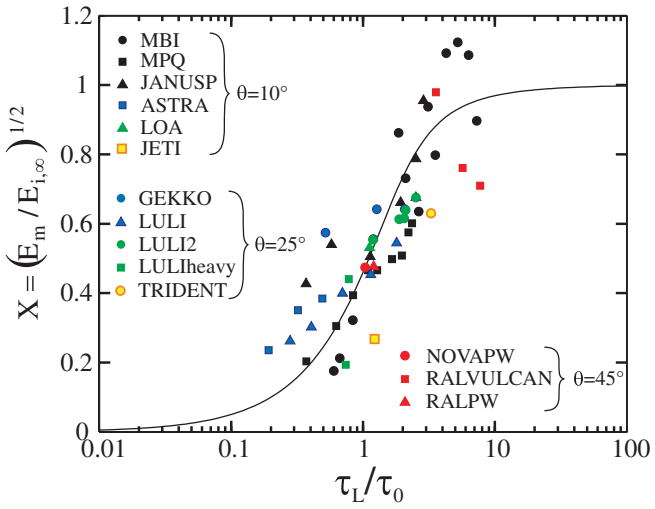

FIG. 1 (color). Comparison of experimental results with theory (solid line). The symbols denote the experimentally obtained maximum ion energies from different laser systems split in three groups with respect to the laser pulse energy: ~1 J (MBI, data presented in Fig. 2, MPQ [9], JANUSP [6], ASTRA [24], LOA [25], JETI [26]); ~10 J (GEKKO [27], LULI and LULI2 [16], LULIheavy [21], TRIDENT [28]); and ≳ 100 J (RALPW [29], RALVULCAN [19], NOVAPW [4]). A single value of θ is assigned to each group. All data refer to protons, except Ref. [21], where also C^{4+} and F^{7+} ions were accelerated, and Ref. [28], where monoenergetic C^{5+} ions were observed.

uncertainty even of a factor of 2 might be realistic. Since B enters the time τ_0 only, such an uncertainty would be reflected in a horizontal displacement of data points in Fig. 1 by the same amount and thus lies within the general scatter of the experimental data. Regarding the range of parameters, the comparison presented in Fig. 1 shows a remarkably good agreement with our theory and thus supports its generality.

Regarding the power dependence of Eq. (8), the final ion energy $E_{i,\infty}$ could be increased for laser systems with constant pulse energy E_L by shortening the pulse duration τ_L. However, short laser pulse duration means a reduction of the acceleration time so that massive ions cannot reach the final energy any more. That this effect is of practical relevance is demonstrated in Fig. 2, where E_m is given as a function of pulse duration for four fixed laser energies E_L (solid lines). It is evident that the highest ion energies E_m^{opt} are obtained for an optimum value τ_L^{opt}. In addition, Fig. 2 reveals that for ion acceleration it is not favorable to build a petawatt laser with pulse duration smaller than about 100 fs for the chosen set of parameters. On the other hand, keeping the laser power P_L constant while increasing E_L and τ_L does not result in an increase of the maximum ion energy once the optimal pulse duration τ_L^{opt} is exceeded. This saturation effect ($E_m = E_{i,\infty}$ for $\tau_L \rightarrow \infty$ visible in the slope of the shaded area in Fig. 1) was also observed in recent PIC simulations [20]. In order to test our approach, an experiment at the 10 Hz-Ti:Sa-laser system of the Max-Born-Institut, Berlin, was performed. The laser energy E_L was 0.7 J within a focal spot of 8 μm (FWHM). Both parameters were kept constant while the laser pulse duration τ_L was changed between 50 fs and 5 ps. Clearly, the experimental data points in Fig. 2 reveal the existence of an optimal pulse duration τ_L^{opt} of about 250 fs, well in agreement with the prediction of our model.

The left graph in Fig. 3 depicts the optimal laser pulse duration τ_L^{opt} for varying laser energy E_L. The nonmonotonic behavior of τ_L^{opt} results from the explicit intensity dependence of the conversion efficiency. An intensity independent η would result in a strictly decreasing function. The solid line in the right graph in Fig. 3 illustrates the maximum proton energy E_m^{opt} that can be achieved under optimum conditions as a function of the laser pulse power $P_L = E_L/\tau_L^{\mathrm{opt}}$. It shows the same dependence on the laser power as $E_{i,\infty}$ [dotted line, Eq. (8)], a scaling that is corroborated by recent PIC simulations [20].

In a minority of laser ion acceleration experiments, the contaminating hydrogen layer was removed from the target surfaces [21,22], thus allowing for the observation of the acceleration of heavier ions. This immediately implies the question of how the acceleration process depends on the ion charge $q_i e$. Experimentally, this issue has been investigated by Schreiber *et al.* [22]. Not touching the nontrivial problem of describing the charge state population, we assume that all charge states q_i are generated close to the rear surface and are then accelerated in the same electric field. Figure 4 shows the maximum ion energy as a function of charge state for a variety of ions. Since in the experiment cited [22] all ions have been accelerated under identical experimental conditions (i.e., constant E_L, τ_L, r_L, d, and θ), it can be readily seen from Eq. (9) that in this case the scaled ion energy E_m/A_i is a unique function of q_i/A_i, where A_i is the ion nucleon number. The solid curve in Fig. 4 represents this function and shows a fair agreement with experimental data ranging from Li to W ions.

It seems to be indicated to compare our result of Eq. (9) with that of PEM [13,16]

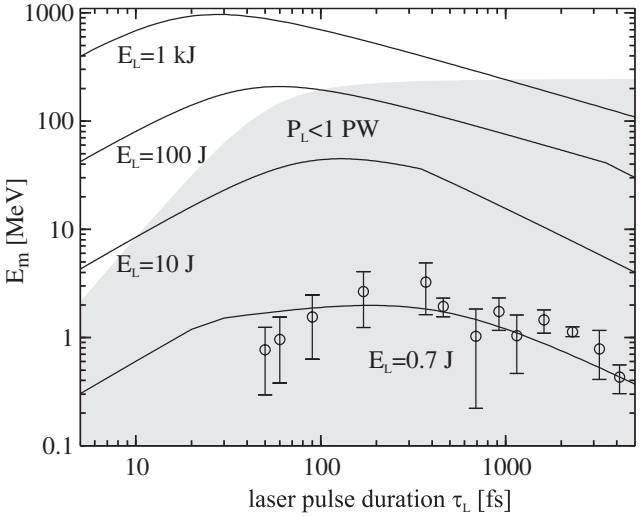

FIG. 2. Dependence of maximum proton energies E_m on the laser pulse duration τ_L for four constant laser energies E_L. The circles represent the experimental data. All four curves (solid lines) correspond to $r_L = 4$ μm, $d = 10$ μm, and $\theta = 10°$. The gray shaded area denotes the region where the laser pulse power P_L is smaller than 1 PW.

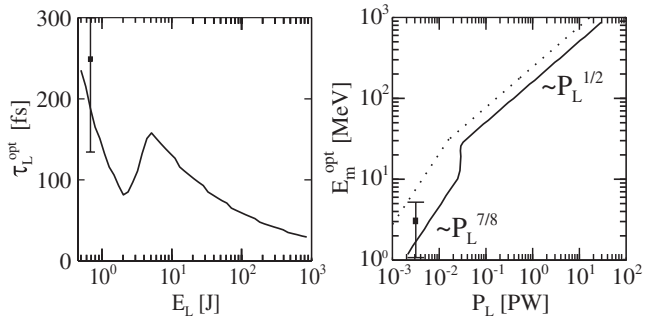

FIG. 3. Dependence of the optimal pulse duration τ_L^{opt} on the laser energy E_L (left). The parameters are identical to those in Fig. 2. The right graph shows the maximum energies E_m^{opt} (solid line) and $E_{i,\infty}$ (dotted line) for optimal laser powers $P_L = E_L/\tau_L^{\mathrm{opt}}$. The data points depict the experimental results derived from Fig. 2.

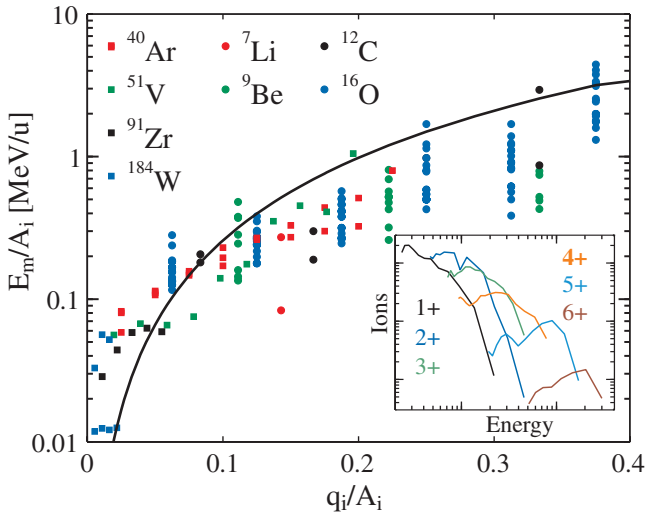

FIG. 4 (color). Scaled maximum ion energies vs charge-to-mass ratios q_i/A_i. The data for fixed ratios result from different laser shots and thus give a measure of the reproducibility from shot to shot. The solid curve is obtained from Eq. (9). For illustration, the inset shows charge state resolved energy spectra in the case of oxygen.

$$E_m^{\mathrm{PEM}} = 2q_i k_B T_e [\ln(\tau + \sqrt{\tau^2 + 1})]^2, \qquad (10)$$

where $\tau = 0.43\omega_{pi}\tau_L$. The ion plasma frequency is given by $\omega_{pi} = (n_{i0}(q_i e)^2/\epsilon_0 m_i)^{1/2}$, where n_{i0} is the plasma ion density before expansion. A natural choice of n_{i0} is the atom solid state density of typically $10^{23}/\mathrm{cm}^3$. Combined with an expression for the hot electron temperature T_e given by Wilks *et al.* [23], the obtained maximum ion energies would differ from experimental data by about an order of magnitude. Attempts to circumvent this problem have been made by Kaluza *et al.* [9] and Fuchs *et al.* [16]. However, in our model, no detailed description of the plasma is needed and the relevant characteristic constant is the ballistic time $\tau_0 = B/v(\infty)$, which is independent of the ion density. This seems to be an advantage in cases where ions from surface contaminants are considered. We also note that the maximum ion energy of Eq. (10) diverges logarithmically for large pulse durations τ_L, in contrast to the saturation effect discussed above.

In conclusion, our model describes in good agreement the maximum ion energies observed nowadays in high-intensity laser experiments with foil targets, including those where different charge-to-mass ratios are present. We have found that the highest intensity is not necessarily suitable for reaching maximum ion energies.

This work was supported by DFG under Contract No. TR18.

*Electronic address: joerg.schreiber@mpq.mpg.de

[1] A. P. Fews *et al.*, Phys. Rev. Lett. **73**, 1801 (1994).
[2] A. Maksimchuk, S. Gu, K. Flippo, D. Umstadter, and V. Y. Bychenkov, Phys. Rev. Lett. **84**, 4108 (2000).
[3] E. L. Clark *et al.*, Phys. Rev. Lett. **84**, 670 (2000).
[4] R. A. Snavely *et al.*, Phys. Rev. Lett. **85**, 2945 (2000).
[5] S. P. Hatchett *et al.*, Phys. Plasmas **7**, 2076 (2000).
[6] A. J. Mackinnon *et al.*, Phys. Rev. Lett. **88**, 215006 (2002).
[7] F. N. Beg *et al.*, Phys. Plasmas **4**, 447 (1997).
[8] E. L. Clark *et al.*, Phys. Rev. Lett. **85**, 1654 (2000).
[9] M. Kaluza *et al.*, Phys. Rev. Lett. **93**, 045003 (2004).
[10] S. C. Wilks *et al.*, Phys. Plasmas **8**, 542 (2001).
[11] A. Pukhov, Phys. Rev. Lett. **86**, 3562 (2001).
[12] J. E. Crow, P. L. Auer, and J. E. Allen, J. Plasma Phys. **14**, 65 (1975).
[13] P. Mora, Phys. Rev. Lett. **90**, 185002 (2003); Phys. Rev. E **72**, 056401 (2005).
[14] J. Yu *et al.*, Phys. Plasmas **6**, 1318 (1999).
[15] M. H. Key *et al.*, Phys. Plasmas **5**, 1966 (1998).
[16] J. Fuchs *et al.*, Nature Phys. **2**, 48 (2006).
[17] S. V. Bulanov *et al.*, in *The Physics of Ionized Gases: 22nd Summer School and International Symposium on the Physics of Ionized Gases*, edited by L. Hadžievski, T. Grozdanov, and N. Bibic, AIP Conf. Proc. No. 740 (AIP, New York, 2004), p. 414.
[18] J. Fuchs *et al.*, Phys. Rev. Lett. **91**, 255002 (2003).
[19] M. Zepf *et al.*, Phys. Plasmas **8**, 2323 (2001).
[20] T. Esirkepov, M. Yamagiwa, and T. Tajima, Phys. Rev. Lett. **96**, 105001 (2006).
[21] M. Hegelich *et al.*, Phys. Rev. Lett. **89**, 085002 (2002).
[22] J. Schreiber *et al.*, Appl. Phys. B **79**, 1041 (2004).
[23] S. C. Wilks, W. L. Kruer, M. Tabak, and A. B. Langdon, Phys. Rev. Lett. **69**, 1383 (1992).
[24] I. Spencer *et al.*, Phys. Rev. E **67**, 046402 (2003).
[25] S. Fritzler *et al.*, Appl. Phys. Lett. **83**, 3039 (2003).
[26] H. Schwoerer *et al.*, Nature (London) **439**, 445 (2006).
[27] Y. Murakami *et al.*, Phys. Plasmas **8**, 4138 (2001).
[28] B. M. Hegelich *et al.*, Nature (London) **439**, 441 (2006).
[29] P. McKenna *et al.*, Phys. Rev. E **70**, 036405 (2004).